Impact of tides on non-coplanar orbits of progenitors of high-mass X-ray binaries

A. Simaz Bunzel[*,1,2], F. García[1,2], J. A. Combi[1,2,3], F. Fortin[4], and S. Chaty[4]

[1] Instituto Argentino de Radioastronomía (CCT La Plata, CONICET; CICPBA; UNLP), C.C.5, (1894) Villa Elisa, Buenos Aires, Argentina
[2] Facultad de Ciencias Astronómicas y Geofísicas, Universidad Nacional de La Plata, Paseo del Bosque, B1900FWA La Plata, Argentina
[3] Departamento de Ingeniería Mecánica y Minera (EPSJ), Universidad de Jaén, Campus Las Lagunillas s/n Ed. A3, E-23071 Jaén, Spain
[4] Université Paris Cité, CNRS, Astroparticule et Cosmologie, F-75013 Paris, France

ABSTRACT

Context. An important stage in the evolution of massive binaries is the formation of a compact object in the system. It is believed that in some cases a momentum kick is imparted to the newly born object, changing the orbital parameters of the binary, such as eccentricity and orbital period, and even acquiring an asynchronous orbit between its components. In this situation, tides play a central role in the evolution of these binaries.
Aims. In this work we aim to study how the orbital parameters of a massive binary change after the formation of a compact object when the stellar spin of the non-degenerate companion is not aligned with the orbital angular momentum.
Methods. We used MESA, which we modified to be able to evolve binaries with different values of the inclination between the orbital planes before and just after the formation of the compact object. These modifications to the equations solved by the MESA code are extended to the case of non-solid body rotation.
Results. We find that the impact of having different initial inclinations is mostly present in the evolution towards an equilibrium state that is independent of the inclination. If the binary separation is small enough such that the interaction happens when the star is burning hydrogen in its core, this state is reached before the beginning of a mass-transfer phase, while for a wider binary not all conditions characterizing the equilibrium are met. We also explore the effect of having different initial rotation rates in the stars and how the Spruit-Tayler dynamo mechanism affects the angular momentum transport for a non-coplanar binary.
Conclusions. These findings show that including the inclination in the equations of tidal evolution to a binary after a kick is imparted onto a newly born compact object changes the evolution of some parameters, such as the eccentricity and the spin period of the star, depending on how large this inclination is. Moreover, these results can be used to match the properties of observed X-ray binaries to estimate the strength of the momentum kick.

Key words. (stars:) binaries (including multiple): close – stars: evolution – X-rays: binaries

1. Introduction

Tidal evolution operates in a binary system by changing both orbital and rotational parameters of its components. In a closed binary system, the conservation of angular momentum (AM) leads to an exchange of AM between the orbit and the stars, which tends to an equilibrium state characterized by a circular orbit (circularization), with stars rotating at a rate equal to the orbital motion (synchronous orbit), and with their spin axes parallel to the orbital AM (coplanarity). Moreover, tides are tightly correlated to the separation in the binary such that the closer the components of a binary are, the stronger the tides acting on it will be, thus causing faster evolution to the equilibrium state. Furthermore, the strength of the tidal interaction depends on the physical process responsible for the dissipation of kinetic energy (Zahn 2008). In reality, binaries are not closed systems and a sink of AM is present in the form of stellar winds, gravitational radiation, and even inefficient mass-transfer (Landau & Lifshitz 1975;

Soberman et al. 1997), so that binaries can only attain equilibrium conditions for a brief period of time.

In particular, the evolution of tides is of great importance for the progenitors of X-ray binaries (XRBs), composed by a non-degenerate star interacting with a compact object, and for double compact object (DCO) systems. The compact object, which can either be neutron star (NS) or a black hole (BH), is formed at the end of the evolution of a massive star due to the unavoidable collapse of its outer layers onto its central regions, driven by the overwhelming gravitational attraction (Hoyle & Fowler 1960; Janka 2012). During this stage some ejection of mass can naturally impart a momentum kick to the newly formed compact object obtained from linear momentum conservation (Blaauw 1961). Furthermore, an asymmetry present during the collapse phase can also lead to a change in the orbital parameters (Kalogera 1996). The origin of these asymmetries may be related to either neutrino emission (Scheck et al. 2006, and references therein) or to mass ejection during the supernova (SN) caused by rotation in the collapsing core (Kotake et al. 2003), hydrodynamic instabilities, magnetic fields, or convective motions (Herant et al. 1994; Burrows et al. 1995; Janka & Mueller

---

[*] Fellow of CONICET

1996; Keil et al. 1996). The necessity of this asymmetry lies in observations of young isolated pulsars with space velocities as high as 400 km s^{-1} (Hobbs et al. 2005), too high to have been born from the breakup of a binary system in a SN explosion. After these changes take place in a binary, the new configuration will be out of equilibrium and the orbit will become eccentric in addition to having some degree of asynchronous orbit between the components. It is in these cases that tides will operate to find a new equilibrium condition.

On the one hand, tides are believed to replenish the AM of a star, spinning it up and potentially becoming able to produce rapidly rotating compact objects (Qin et al. 2019; Belczynski et al. 2020; Fishbach & Kalogera 2021). There is a hint that this mechanism operates on the observed population of high-mass XRBs (HMXBs) containing a BH, as measurements of BH spins show high values (Miller & Miller 2015), although these measurements relay on model-dependent fits (Belczynski et al. 2021). It is worth mentioning that Qin et al. (2022a) have recently found that allowing for a regime of hypercritical accretion can explain at least one case of a rapidly rotating BH in a HMXB. On the other hand, most of the spins of BHs measured by the LIGO and Virgo collaboration (Abbott et al. 2021) are small. It is believed that in these cases the tides are not strong enough to cause a spin up of the stars and an efficient AM transport leads to slowly rotating compact objects (Qin et al. 2018; Olejak & Belczynski 2021; Qin et al. 2022b). Moreover, some models for long gamma-ray bursts require rapidly rotating massive stars at the end of their evolution (Woosley 1993; Paczyński 1998), which could be achieved thanks to the spin up of the progenitor stars due to the action of tides. Thus, it is clear that the interplay between tides and AM transport takes a fundamental role in shaping the different outcomes of the evolution of massive binaries containing compact objects.

Most of the works in which tidal evolution is implicitly considered assume that coplanarity is instantly achieved, and only follow numerically the evolution towards a circular and synchronous orbit. This approach is based on the fact that the timescales for each equilibrium condition are different to each other, with coplanarity being reached faster than the rest. However, a difference might still be present when considering the effect of non-zero inclinations in the equations of tidal evolution. In this work, our aim is to understand the role that noncoplanarity plays in the evolution of different binary parameters of the immediate progenitors of HMXBs. In order to do so, we consider the set of differential equations of tidal evolution derived by Repetto & Nelemans (2014), which we incorporate in the publicly available stellar evolution code `MESA`. Before using it to analyse the evolution of HMXBs, we compare our code with the outcome of other codes in the literature. The paper is organized as follows: in Section 2 we describe the model used together with the additions included in the stellar evolution code. In Section 3 we present the results of some exemplary cases of study. We present a summary of our findings and concluding remarks in Section 4.

2. Methods

2.1. Tidal modelling

Orbital parameters can be modified as a consequence of tides operating in a binary. These tidal forces, which are present in the surface of a stellar component, will not be aligned with a line joining the centre of the components of the binary, due to different mechanisms of energy dissipation, thus producing a torque

in the system. Then, thanks to the spin-orbit coupling, tidal interactions can modify the orbital AM as well as the spin of the components of the binary. Hence, to understand how these tides operate in a binary, it is important to have a model to account for their evolution.

In order to model the effect of tides acting on a non-coplanar progenitor of a HMXB, we consider the equations presented in Repetto & Nelemans (2014) which are valid for arbitrary inclinations between the stellar spin and the orbital AM. That work was an extension of the tidal-interaction study presented in Hut (1981), where only small-angle deviations were considered. In this work we combine those equations with the adjustments described in Paxton et al. (2015) to include the case of differentially rotating stars, in which the AM is distributed throughout the entire stellar interior and envelope.

This particular model of tidal evolution, where only tides with a small deviation from the equilibrium shape are considered, is called the weak friction model (see e.g. Darwin 1879; Alexander 1973). Here it is assumed that the deviation of tides in magnitude and direction are parametrized by a constant time lag, thus allowing for slow variations of orbital parameters within an orbital period. Dynamical effects, in which stars can oscillate, are not considered. For a review of these dynamical effects, see Zahn (1977).

Coupled with the stellar evolution of the binary, the tidal equations to solve are

$$
\frac{da}{dt} = -6 \left(\frac{K}{T}\right)_1 q(1+q) \left(\frac{R_1}{a}\right)^8 \frac{a}{(1-e^2)^{15/2}} \left[f_1(e^2) - (1-e^2)^{3/2} f_2(e^2) \frac{\Omega_1 \cos i}{\Omega_{\rm orb}}\right],
\tag{1}
$$

$$
\frac{de}{dt} = -27 \left(\frac{K}{T}\right)_1 q(1+q) \left(\frac{R_1}{a}\right)^8 \frac{e}{(1-e^2)^{13/2}} \left[f_3(e^2) - \frac{11}{8} (1-e^2)^{3/2} f_4(e^2) \frac{\Omega_1 \cos i}{\Omega_{\rm orb}}\right],
\tag{2}
$$

$$
\frac{d\Omega_1}{dt} = -3 \left(\frac{K}{T}\right)_1 \frac{q^2}{k^2} \left(\frac{R_1}{a}\right)^6 \frac{\Omega_{\rm orb}}{(1-e^2)^6} \left[f_2(e^2) \cos i - \frac{\Omega_1}{4\,\Omega_{\rm orb}} (1-e^2)^{3/2} (3+2\cos 2i) f_5(e^2) \frac{\Omega_1 \cos i}{\Omega_{\rm orb}}\right],
\tag{3}
$$

$$
\frac{di}{dt} = -3 \left(\frac{K}{T}\right)_1 \frac{q^2}{k^2} \left(\frac{R_1}{a}\right)^6 \frac{\Omega_{\rm orb} \sin i}{\Omega_1 (1-e^2)^6} \left[f_2(e^2) - \frac{f_5(e^2)}{2}\right] \times \left(\frac{\Omega_1 \cos i\,(1-e^2)^{3/2}}{\Omega_{\rm orb}} + \frac{R_1^2\,a\,\Omega_1^2\,k_1^2\,(1-e^2)}{M_2\,G}\right).
\tag{4}
$$

Here the sub-indices 1 and 2 refer to the non-degenerate star and the compact companion, respectively. The term $(K/T)_1$ is a measure of the strength of the tidal dissipation, with K being the apsidal motion constant and T the timescale at which changes in the orbit occur due to tides. The mass ratio (q) is defined as $q = M_2/M_1$; k is the radius of gyration of the star, equal to $k = I/(M R)^2$ with I being the moment of inertia of the star; and $f_i(e^2)$ are the polynomials of the eccentricity, e, as presented in Hut (1981); and Ω_1 is the rotational velocity of the star, while $\Omega_{\rm orb}$ is the orbital angular velocity. The equations show the strong dependence with the orbital separation (a), coupled with

the radius of the star (R_1), as well as the role of the inclination (i) between the orbital and the star angular momenta.

The term K/T depends on the source of dissipation of kinetic energy, in which T is a characteristic timescale for that source of dissipation. For stars with a convective envelope, this source is the turbulent convection, so that T is the eddy turnover timescale. For this type of stars we consider a calibration factor of

$$\left(\frac{K}{T}\right)_1 = \frac{2}{21} \frac{f_{\mathrm{conv}}}{\tau_{\mathrm{conv}}} \frac{M_{\mathrm{env}}}{M_1}, \qquad (5)$$

where f_{conv} is the fraction of convective cells that contribute to the damping, for which we assume a quadratic dependence with the tidal-forcing frequency (Goldreich & Nicholson 1977), increased by a factor of 50 (Belczynski et al. 2008).

In the case of a star with a radiative envelope, dissipation is assumed to be produced by radiative damping. We use the calibration factor as in Hurley et al. (2002)

$$\left(\frac{K}{T}\right)_1 = 1.9782 \times 10^4 \frac{M_1 R_1^2}{a^5} (1 + q)^{5/6} E_2, \qquad (6)$$

where E_2 measures the coupling between the tidal potential and gravity mode as given by Zahn (1975).

Although the agreement between the observations and the theoretical predictions of tidal torques is quite satisfactory, the complex physical mechanisms that are at the origin of the tidal torques are not completely understood so that the evaluation of K/T require some calibration factors, as mentioned before. Naturally, given the physical origins of the convective turbulence and the radiative damping, their efficiencies are different with convective envelope stars presenting more tidal friction than those with radiative envelopes.

Then we integrate the set of equations for tidal evolution described above and couple them with the evolution of the orbital AM. Once the value of i is known at a given timestep from solving Equation 4, we use the hooks provided by the `MESA` code for the following: the `other_edot_tidal` subroutine is used to solve the evolution of e, while the `other_sync_spin_to_orbit` subroutine computes the tidal torque acting on the non-degenerate companion.[1]

2.2. Stellar modelling

The detailed evolution of binary systems is computed using the stellar evolution code `MESA` (version 15140, Paxton et al. 2011, 2013, 2015, 2018, 2019). All computed stars are assumed to have a solar metallicity content, $Z = Z_\odot = 0.017$ (Grevesse & Sauval 1998). We use the default nuclear reactions networks present in `MESA`, `basic.net`, `co_burn.net` and `approx21.net`, which are switched dynamically as later stages in the evolution are reached. Convective regions, which are defined according to the Ledoux criterion (Ledoux 1947), are modelled using the standard mixing-length theory (Böhm-Vitense 1958) with a mixing-length parameter $\alpha_{\mathrm{MLT}} = 1.5$. Semi-convection is modelled following Langer et al. (1983) with an efficient parameter $\alpha_{\mathrm{SC}} = 1$. We include convective core overshooting during core hydrogen burning following Brott et al. (2011). In order to avoid some numerical problems during the evolution of massive stars until the Wolf-Rayet (WR) stage, we use the MLT++ formalism,

as presented in Paxton et al. (2013), which reduces the super-adiabaticity in regions where the convective velocities approach the speed of sound. Additionally, the effect of thermohaline mixing, which accounts for the unstable situation arising when material accreted by the accretor has a mean molecular weight higher than its outer layers, follows Kippenhahn et al. (1980) with an efficiency parameter of $\alpha_{\mathrm{th}} = 1$. The modelling of stellar winds follows that of Brott et al. (2011), as described in Marchant et al. (2017). Stellar rotation is modelled following the description of Heger et al. (2000), with composition and angular momentum transport mechanisms including the Eddington-Sweet circulation, secular and dynamical shear instabilities, and the Goldreich-Schubert-Fricke (GSF) instability. Moreover, the impact of magnetic fields on the transport of AM follows the Petrovic et al. (2005) implementation, where the Spruit-Tayler (ST) dynamo is taken into account (Spruit 2002). Whether this dynamo effect should be considered in the transport of AM is the object of a current debate: Qin et al. (2019) have shown that without it models of BHs in HMXBs can reach near critical rotation (spin parameter $a \sim 1$), while models considering its impact in the AM transport leads to BHs with near zero spin values, in contradiction to spin measurements of BHs in HMXBs. In this work we consider models with and without this mechanism operating in the AM transport.

In our models a star is initially assumed to be rotating as a solid body. We explore two different cases for the initial rotation rate: one where the star is rotating at 90% of its critical value, and the other where the star is rotating at 10% of this value. The difference between these two conditions lies in how AM is exchanged between the orbit and the star during the evolution. Moreover, we consider AM losses in the orbit from gravitational wave radiation, mass loss, and spin-orbit coupling, as described in Paxton et al. (2015).
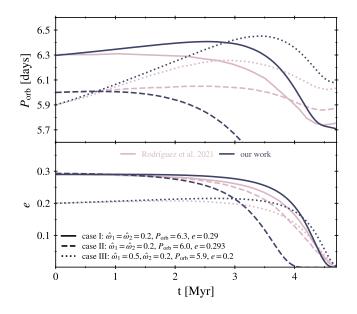
At the start of the calculations, binaries are initially assumed to have already gone through the formation of the compact object, such that some eccentricity is present. In addition, we also consider the binary to be non-coplanar and with asynchronous orbit between the star and the compact object. We also neglect the evolution prior to this point of the interior of the companion star to the compact object, considering that it is represented by a zero age main sequence (ZAMS) star. Binary interaction is computed with the `MESAbinary` module of `MESA`. When the star in the binary overflows its Roche lobe, the mass transfer (MT) rate is implicitly computed following the prescription of Kolb & Ritter (1990). A key factor in the Roche model is the assumption of synchronous orbit, which in our case is not imposed. As we show, in some of our simulations there are cases where the binary is close to a MT stage, but have not yet achieved a synchronous state. Moreover, the model of Hut (1981) considers only quadrupolar terms as a perturbation to a central force field, which for a star nearly filling its Roche lobe might not be the best representation. In this case the tidal coupling should be stronger than predicted. For simplicity, we extend the conditions of the Roche model to asynchronous orbit binaries. However, we caution that this is formally not correct.

In all the cases explored, our simulations are followed until the non-degenerate star reaches the end of the core helium burning phase.

2.3. Validation of the method

Before presenting the results for the progenitors of HMXBs, we computed similar cases to other results present in the modern literature concerning the effect of tides on the evolution of non-

---

[1] The modified version of the code can be found in the following GitHub repository: `https://github.com/asimazbunzel/non-coplanar-tides`

Fig. 1. Comparison of the evolution of the orbital parameters for the different scenarios explored by Rodríguez et al. (2021). Shown in dark blue are the results found with our modifications to the MESA source code, while in grey the results from Rodríguez et al. (2021). In the top (bottom) panel the evolution of P_{orb} (e) is represented for different initial conditions (see legend). All three cases are described in more detail in Rodríguez et al. (2021).
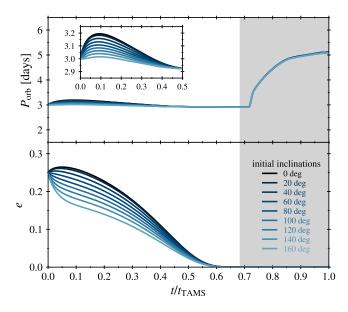
coplanar binaries with the aim of verifying and validating our implementation. To this end, we computed a set of evolutionary models as in Rodríguez et al. (2021) as a comparison. In order to do so, we modified the method described in Section 2.1 to consider the change over time of each of the components of the binary, including both the rotational angular velocity and the inclination of the spin with respect to the orbital AM.

The chosen binary is composed of a 17.9 $M_\odot$ secondary star orbiting around a 33.8 $M_\odot$ primary star, in eccentric orbits with different initial periods, P_{orb}. We computed three models, as Rodríguez et al. (2021) did. These evolutionary tracks were followed until the end of the main sequence (MS) phase.

In Fig. 1 the evolution of P_{orb} and e are presented. For each individual case covering different initial conditions, we are able to find similar behaviours in the overall evolution of the orbital parameters. The main differences are found in the evolution of P_{orb} in the range $1 - 4$ Myr, which could be associated with the different mechanisms of AM losses considered in our model. Around 4 Myr the evolutionary tracks for cases I and III seem to behave in the same manner; during this phase the stars are close to each other, with tides playing an important role in the evolution.

In contrast, for case II we obtain a faster declining P_{orb} evolution. Compared to that work, this deviation starts at around 2 Myr and grows over time. Close to 2.5 Myr the binary achieves coplanarity, while synchronous orbit is reached at 3.8 Myr. Finally, at about 4 Myr the orbit becomes circular. However, our value of P_{orb} is lower than that found by Rodríguez et al. (2021), likely due to differences in how AM is computed in our code with respect to theirs.

In addition, in the bottom panel of Fig. 1 we show that the evolution of e closely resembles the results of Rodríguez et al. (2021) in all the cases. Once again, in case II we find that our simulation evolves towards a circular orbit faster than theirs.

Fig. 2. Main sequence evolution of P_{orb} (top panel) and e (bottom panel). Each shade of blue represents a detailed evolution assuming an initial inclination (see legend, bottom panel). The coplanar case ($i = 0$) is shown in black. The zoomed-in region in the top panel presents a clear picture of the different orbital periods around the first half of the MS evolution of the binaries. The grey region indicates the MT phase.
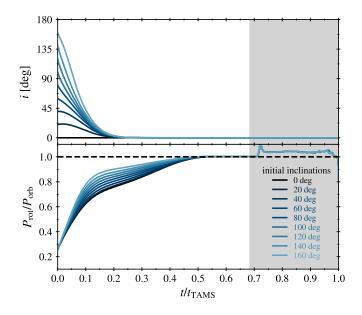
3. Results

In this section, we show the results on the evolution of different binary parameters subject to non-coplanar tides.

3.1. Mass transfer during core hydrogen burning

First, we model the evolution of a progenitor of a HMXB in which the MT between the star and the compact object occurs when the non-degenerate star is in the MS, called case A of MT (Kippenhahn & Weigert 1967). For this, we model a binary consisting of a 15 $M_\odot$ BH in an eccentric orbit with $e = 0.25$ and $P_{orb} = 3$ days, around a 20 $M_\odot$ companion star. The star is assumed to be rotating at 0.9 of its critical rotation rate ($\Omega_1/\Omega_{crit} = 0.9$). To understand the role of non-coplanarity, we explore several different inclinations between the spin of the star and the orbital AM, as well as the coplanar case of ($i = 0$).

The impact of different initial inclinations on P_{orb} and e is shown in Figure 2. It is clear that there is little change in P_{orb} due to the inclination evolution. The most important changes occur at the beginning of the MS evolution of the star, where P_{orb} increases faster for the smaller values of i. However, after half of the MS evolutionary timescale, the differences in P_{orb} disappear. On the other hand, when studying the change in e, we see a clear difference before reaching a MT phase. In this case, inclinations higher than 90 degrees are able to change the slope of the eccentricity derivative, leading to the different shapes shown in the bottom panel of Figure 2. However, in all cases the binary tends to reach the equilibrium state characterized by a circular orbit in less than 70% of the MS evolutionary timescale.

We show the evolution of the inclination between the spin of the star and the orbital AM in Figure 3, which reflects that the slope of i in function of time (t) varies according to its initial value. For all cases, we find that in less than 20% of the MS lifetime of the star the binary reaches coplanarity ($i = 0$), after which the equations derived by Hut (1981) are recovered.

Fig. 3. Evolution during main sequence of i (top panel) and P_{rot}/P_{orb} (bottom panel). Each shade of blue represents a detailed evolution assuming an initial inclination (see legend, bottom panel). The coplanar case ($i = 0$) is shown in black. The case $P_{rot}/P_{orb} = 1$, which represents a synchronous orbit, is shown as a black dashed line. The grey region indicates the MT phase.
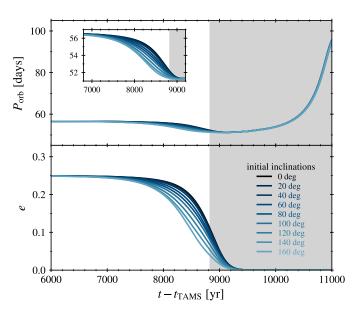

Fig. 4. Same parameter evolutions as in Figure 2, but the time axis starts just after the end of the MS. The evolution of these parameters before ~6 000 yr after reaching the end of the MS is the same in all the different inclination cases. In the zoomed-in region the small differences present in P_{orb} just before the beginning of the MT phase are shown. The grey region indicates the MT phase.

In addition, in Figure 3 we present the evolution towards a synchronous orbit, by showing the ratio of the rotational period of the star, P_{rot}, to P_{orb}. Before reaching the equilibrium state, the rotational rate differs for different values of i, acquiring faster rotations for the smallest inclinations. Here it is clearly seen how this equilibrium condition is achieved at around half of the MS lifetime, thus safely allowing the use of the Roche formalism for the MT stage, which happens at around 70% of the MS lifetime.

From Figs. 2 and 3 we conclude that the non-coplanar tides acting on a tight binary in which its components interact during core-H burning push the binary to reach the equilibrium state before the start of the MT phase that characterizes an accreting HMXB.
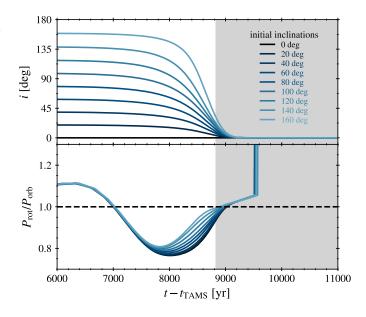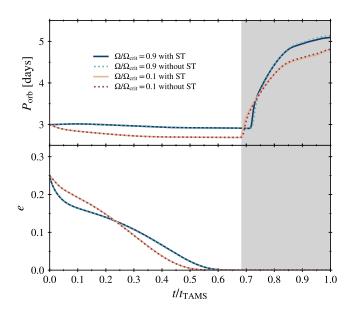
3.2. Mass transfer after core hydrogen depletion

In order to study the impact of tides over a broad range of conditions, we also explore cases with a wider binary configuration. Here we present the results for the evolution of a binary with the same component masses, eccentricities, and rotational rates as in Section 3.1, but with a higher P_{orb} of 50 days. For these cases the beginning of the MT phase occurs after the end of MS evolution, when the star crosses the Hertzsprung gap (HG), such that the MT is commonly referred to as case B of MT (Kippenhahn & Weigert 1967).

The evolution of P_{orb} and e for different values of i are shown in Figure 4. Similar to case A of MT, P_{orb} behaves in an analogous manner for the different i values. There is, however, a small difference just before the start of the MT phase, as highlighted in the inset of the figure. For the evolution of e, shown in the bottom panel of Figure 4, we see that its progress over time depends on the inclination, with smaller values of i favouring smaller changes towards a circular orbit. Hence, for this case of MT a circular orbit is reached a few hundred years after the start of the MT phase, around 9 500 yr after the end of the MS evolution.

Fig. 5. Same parameter evolutions as in Figure 3, but with a time axis as described in Figure 4. The black dashed line represents the synchronous orbit.

Regarding the inclination evolution shown in Figure 5, we see that it starts to change some thousands of years before the beginning of the MT phase, with the more abrupt changes related to the higher initial i values. This behaviour is a consequence of the increase in the radius of the star such that the ratio R_1/a becomes more important in the equations presented in Section 2.1. All these cases tend to a coplanar state that is reached just after the start of the MT phase.

An important result found for this MT case is connected to the evolution of P_{rot}/P_{orb} (see bottom panel of Figure 5). On the

Fig. 6. Same evolution as in Figure 2, but for different conditions in the spin of the star and the AM transport (see legend, top panel).

Fig. 7. Same evolution as in Figure 3, but for different conditions in the spin of the star and the AM transport (see legend, top panel). The black dashed line represents a synchronous orbit.

one hand, we find that $\sim 7\,000$ yr after the end of the MS the star begins to rotate at a faster rate than P_{orb}, but this tendency is reverted during the last thousand years before the start of the MT phase. On the other hand, during the first hundred years of the MT phase, the star does not have a totally synchronous orbit. This equilibrium state is briefly achieved until the clear slow down of the spin of the star occurring around $\sim 9\,500$ yr after the MS.
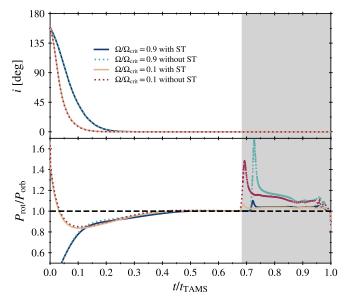
Thus, we can conclude that the different initial values of i reach equilibrium conditions on a similar timescale, but the evolution towards those conditions can be very different, as in the cases of e and $P_{\mathrm{rot}}/P_{\mathrm{orb}}$.

3.3. Different physical assumptions

To explore a wider range of conditions that could modify the evolution of the binaries, we computed a set of models in which the initial binary conditions are fixed, with masses $M_{\mathrm{BH}} = 15\,M_{\odot}$ and $M_1 = 20\,M_{\odot}$, in an eccentric orbit of $e = 0.25$ and $P_{\mathrm{orb}} = 3$ days and an inclination of $i = 80$ deg. We explore two different initial rotation velocities $\Omega_1/\Omega_{\mathrm{crit}} = 0.1, 0.9$, and for each of these cases we turn on and off the contribution of the ST dynamo to the AM transport (respectively labelled in Figure 6 as 'with ST' and 'without ST').

The different results for the evolution of P_{orb} and e are presented in Figure 6. We see that the main difference arises when the initial spins are changed. This behaviour is maintained even after the MT starts as P_{orb} is shorter for the initially less rapidly rotating star. The impact of using the ST dynamo seems to be negligible for these two orbital parameters. In the bottom panel of Figure 6 we show that the condition of circularity is reached first for the slowly rotating case.

However, whether the ST dynamo is considered or not can be seen when studying the evolution of the spin of the star. In Figure 7 we can see this difference in the AM transport becoming important during the MT phase, as the ratio $P_{\mathrm{rot}}/P_{\mathrm{orb}}$ shows a clear change in its value when this contribution is turned on and off.

Overall, the impact of the spin of the star is much more important during the evolution prior to the start of the MT phase, as is expected, due to the explicit dependence in the tidal equations (2.1). Instead, the AM transport becomes relevant once the MT has started, and the binary has reached the equilibrium state.

4. Summary and conclusions

At the end of their evolution, most massive stars go through a core collapse to form a compact object, which could be a NS or a BH. This formation is often associated with very powerful astrophysical transients such as supernovae and gamma-ray bursts. Many physical processes operating during this short-lived stage still remain unknown, one important process being whether this core collapse is symmetric or not. This dichotomy can be seen in the momentum kick imparted to the newly born object, although the presence of this kick may depend on the nature of the compact object, with NSs having well-constrained kick magnitudes (Hobbs et al. 2005), while kicks in BHs are more uncertain (Brandt et al. 1995; Willems et al. 2005; Wong et al. 2012, 2014; Vanbeveren et al. 2020; Callister et al. 2021; Stevenson 2022). In addition, if these stars are members of binary systems, the momentum kick imparted to the remnant will, through linear momentum conservation, modify the orbital parameters of the binary: P_{orb}, e, and i. After that, the orbital and internal AM evolution will be dominated by the effect of tides operating on the binary system.

In this work we address the topic of how these tides operate on the progenitors of HMXBs in which, after such an asymmetric kick is imparted, the spin of the star is not aligned with the orbital AM. For this purpose, we include the formulation of Repetto & Nelemans (2014) for arbitrary inclinations in the stellar evolution code MESA. With this tool, we study the evolution of the binary parameters considering different initial values of the inclination between the AM of the star and the orbital plane i for cases A and B of MT (Kippenhahn & Weigert 1967).

For the evolution through both cases of MT, we note that the most noticeable differences arise in the evolution of e, i, and P_{rot}.

The changes in these parameters are driven by tidal coupling, which forces the system to evolve towards an equilibrium state characterized by circularization, coplanarity, and synchronous orbit. This state is achieved faster for the more compact binary (i.e. the conditions of case A of MT) as a consequence of the strong dependence of tides with the separation between the binary members (see Section 2.1).

Furthermore, in this work we explored the role of the initial spin on the subsequent binary evolution. We find the spin to be an important variable that regulates the timescale for each of the different conditions of the equilibrium state. We also study an important yet debated mechanism of AM transport: the ST dynamo. As already shown by other authors (Qin et al. 2019) its absence could help to explain the high spin measured in the BHs of HMXBs, although this might not be consistent with the population of BHs detected by the LIGO and Virgo collaboration (Abbott et al. 2021). In this work we find that the role of this mechanism is secondary when analysing the change on the binary parameters due to tidal evolution, although it becomes important once a binary reaches the onset of a MT phase. However, the ST dynamo might play an important role in scenarios where a rapidly rotating core of a star is needed at the end of the evolution to reproduce energetic transient events (Fuller & Lu 2022).

Many physical uncertainties could affect our results across this modelling. Understanding the impact of such limitations is a key factor. On the one hand, the set of non-linear differential equations that describe the evolution of the semi-major axis, eccentricity, rotation rate, and inclination of the rotation axis with respect to the orbital plane, as presented by Repetto & Nelemans (2014), is considered until the onset of a MT phase. Once a star is near to filling its Roche lobe, the quadrupolar terms in the perturbation theory of tides of Hut (1981) might stop being a good approximation, with tides becoming stronger than predicted. Moreover, the Roche formalism requires synchronous orbit between the components of the binary and P_{orb}; in our case B of MT, we find small deviations of the synchronous orbit state at the beginning of the MT phase which is rapidly achieved during the first years of MT. Lastly, the transport of AM is also uncertain and will certainly have an impact on the results during the MT phase. There is observational evidence that this transport is highly efficient such that most stars end their evolution with a smaller content of AM than predicted (Cantiello et al. 2014; Fuller et al. 2014; Spada et al. 2016; Aerts et al. 2019; Fuller et al. 2019; Eggenberger et al. 2019; den Hartogh et al. 2019). Although this is particularly true for measurements of BHs with low spin values (Abbott et al. 2021), there seem to be HMXBs containing BHs with high spin values (Miller & Miller 2015). This issue is currently under debate (Qin et al. 2019; Bavera et al. 2020; Fishbach & Kalogera 2021; Belczynski et al. 2021).

The results of this study show that prior to the X-ray binary phase, the evolution of the orbital parameters differ according to the value of the inclination of the rotational axis with respect to the orbital plane. Thus, for some binaries, matching observed quantities with those coming from stellar evolution simulations might help constrain the conditions at core collapse, as well as the momentum kick imparted to the newly born compact object.

Software: MESA[2] (Paxton et al. 2011, 2013, 2015, 2018, 2019), ipython/jupyter (Kluyver et al. 2016), matplotlib (Hunter 2007), numpy (Harris et al. 2020).

References

Abbott, R., Abbott, T. D., Abraham, S., et al. 2021, Physical Review X, 11, 021053
Aerts, C., Mathis, S., & Rogers, T. M. 2019, ARA&A, 57, 35
Alexander, M. E. 1973, Ap&SS, 23, 459
Bavera, S. S., Fragos, T., Qin, Y., et al. 2020, A&A, 635, A97
Belczynski, K., Done, C., & Lasota, J. P. 2021, arXiv e-prints, arXiv:2111.09401
Belczynski, K., Kalogera, V., Rasio, F. A., et al. 2008, ApJS, 174, 223
Belczynski, K., Klencki, J., Fields, C. E., et al. 2020, A&A, 636, A104
Blaauw, A. 1961, Bull. Astron. Inst. Netherlands, 15, 265
Böhm-Vitense, E. 1958, ZAp, 46, 108
Brandt, W. N., Podsiadlowski, P., & Sigurdsson, S. 1995, MNRAS, 277, L35
Brott, I., de Mink, S. E., Cantiello, M., et al. 2011, A&A, 530, A115
Burrows, A., Hayes, J., & Fryxell, B. A. 1995, ApJ, 450, 830
Callister, T. A., Farr, W. M., & Renzo, M. 2021, ApJ, 920, 157
Cantiello, M., Mankovich, C., Bildsten, L., Christensen-Dalsgaard, J., & Paxton, B. 2014, ApJ, 788, 93
Darwin, G. H. 1879, Philosophical Transactions of the Royal Society of London Series I, 170, 1
den Hartogh, J. W., Eggenberger, P., & Hirschi, R. 2019, A&A, 622, A187
Eggenberger, P., Deheuvels, S., Miglio, A., et al. 2019, A&A, 621, A66
Fishbach, M. & Kalogera, V. 2021, arXiv e-prints, arXiv:2111.02935
Fuller, J., Lecoanet, D., Cantiello, M., & Brown, B. 2014, ApJ, 796, 17
Fuller, J. & Lu, W. 2022, MNRAS, 511, 3951
Fuller, J., Piro, A. L., & Jermyn, A. S. 2019, MNRAS, 485, 3661
Goldreich, P. & Nicholson, P. D. 1977, Icarus, 30, 301
Grevesse, N. & Sauval, A. J. 1998, Space Sci. Rev., 85, 161
Harris, C. R., Millman, K. J., van der Walt, S. J., et al. 2020, Nature, 585, 357
Heger, A., Langer, N., & Woosley, S. E. 2000, ApJ, 528, 368
Herant, M., Benz, W., Hix, W. R., Fryer, C. L., & Colgate, S. A. 1994, ApJ, 435, 339
Hobbs, G., Lorimer, D. R., Lyne, A. G., & Kramer, M. 2005, MNRAS, 360, 974
Hoyle, F. & Fowler, W. A. 1960, ApJ, 132, 565
Hunter, J. D. 2007, Computing in Science & Engineering, 9, 90
Hurley, J. R., Tout, C. A., & Pols, O. R. 2002, MNRAS, 329, 897
Hut, P. 1981, A&A, 99, 126
Janka, H.-T. 2012, Annual Review of Nuclear and Particle Science, 62, 407
Janka, H. T. & Mueller, E. 1996, A&A, 306, 167
Kalogera, V. 1996, ApJ, 471, 352
Keil, W., Janka, H. T., & Mueller, E. 1996, ApJ, 473, L111
Kippenhahn, R., Ruschenplatt, G., & Thomas, H. C. 1980, A&A, 91, 175
Kippenhahn, R. & Weigert, A. 1967, ZAp, 65, 251
Kluyver, T., Ragan-Kelley, B., Pérez, F., et al. 2016, in Positioning and Power in Academic Publishing: Players, Agents and Agendas, ed. F. Loizides & B. Scmidt (IOS Press), 87–90
Kolb, U. & Ritter, H. 1990, A&A, 236, 385
Kotake, K., Yamada, S., & Sato, K. 2003, ApJ, 595, 304
Landau, L. D. & Lifshitz, E. M. 1975, The classical theory of fields
Langer, N., Fricke, K. J., & Sugimoto, D. 1983, A&A, 126, 207
Ledoux, P. 1947, ApJ, 105, 305
Marchant, P., Langer, N., Podsiadlowski, P., et al. 2017, A&A, 604, A55
Miller, M. C. & Miller, J. M. 2015, Phys. Rep., 548, 1
Olejak, A. & Belczynski, K. 2021, ApJ, 921, L2
Paczyński, B. 1998, ApJ, 494, L45
Paxton, B., Bildsten, L., Dotter, A., et al. 2011, ApJS, 192, 3
Paxton, B., Cantiello, M., Arras, P., et al. 2013, ApJS, 208, 4
Paxton, B., Marchant, P., Schwab, J., et al. 2015, ApJS, 220, 15
Paxton, B., Schwab, J., Bauer, E. B., et al. 2018, ApJS, 234, 34
Paxton, B., Smolec, R., Schwab, J., et al. 2019, ApJS, 243, 10
Petrovic, J., Langer, N., Yoon, S. C., & Heger, A. 2005, A&A, 435, 247
Qin, Y., Fragos, T., Meynet, G., et al. 2018, A&A, 616, A28
Qin, Y., Marchant, P., Fragos, T., Meynet, G., & Kalogera, V. 2019, ApJ, 870, L18
Qin, Y., Shu, X., Yi, S., & Wang, Y.-Z. 2022a, arXiv e-prints, arXiv:2201.05611
Qin, Y., Wang, Y.-Z., Wu, D.-H., Meynet, G., & Song, H. 2022b, ApJ, 924, 129

---

[2] http://mesa.sourceforge.net/

Repetto, S. & Nelemans, G. 2014, MNRAS, 444, 542

Rodríguez, C. N., Ferrero, G. A., Benvenuto, O. G., et al. 2021, MNRAS, 508, 2179

Scheck, L., Kifonidis, K., Janka, H. T., & Müller, E. 2006, A&A, 457, 963

Soberman, G. E., Phinney, E. S., & van den Heuvel, E. P. J. 1997, A&A, 327, 620

Spada, F., Gellert, M., Arlt, R., & Deheuvels, S. 2016, A&A, 589, A23

Spruit, H. C. 2002, A&A, 381, 923

Stevenson, S. 2022, ApJ, 926, L32

Vanbeveren, D., Mennekens, N., van den Heuvel, E. P. J., & Van Bever, J. 2020, A&A, 636, A99

Willems, B., Henninger, M., Levin, T., et al. 2005, ApJ, 625, 324

Wong, T.-W., Valsecchi, F., Ansari, A., et al. 2014, ApJ, 790, 119

Wong, T.-W., Valsecchi, F., Fragos, T., & Kalogera, V. 2012, ApJ, 747, 111

Woosley, S. E. 1993, ApJ, 405, 273

Zahn, J. P. 1975, A&A, 41, 329

Zahn, J. P. 1977, A&A, 57, 383

Zahn, J. P. 2008, in EAS Publications Series, Vol. 29, EAS Publications Series, ed. M. J. Goupil & J. P. Zahn, 67–90